Journal of Photochemistry and Photobiology A: Chemistry 218 (2011) 204–212

Contents lists available at ScienceDirect

Journal of Photochemistry and Photobiology A: Chemistry

journal homepage: www.elsevier.com/locate/jphotochem

Photophysics and photochemistry of positionally isomeric 1,2-dianthryltetramethyldisilanes: Investigation of anthryl–anthryl and anthryl–SiSi interactions

Koji Takahashi [a], Yoshinobu Nishimura [b], Tatsuo Arai [b], Shiki Yagai [a], Akihide Kitamura [a], Takashi Karatsu [a,*]

[a] Department of Applied Chemistry and Biotechnology, Graduate School of Engineering, Chiba University, 1-33 Yayoi-cho, Inage-ku, Chiba 263-8522, Japan
[b] Department of Chemistry, University of Tsukuba, Tsukuba, Ibaraki 305-8571, Japan

ARTICLE INFO

Article history:
Received 4 October 2010
Received in revised form
16 December 2010
Accepted 31 December 2010
Available online 4 January 2011

Keywords:
Disilane
Fluorescence
Excimer
Rotamer
Single photon counting method

ABSTRACT

Aryldisilanes composed of one or two anthryl groups and tetra- or pentamethyldisilane chain units were prepared. The substitution of disilanes on the two anthryl groups was isomeric at positions 1, 2, and 9 for **1A2S2**, **2A2S2**, and **9A2S2**, respectively. The photochemical properties of these compounds, such as absorption and fluorescence, were studied in solution. The dependence of the intramolecular π–π and σ–π interactions on the substitution position of the anthryl group were examined. The dianthryldisilanes displayed excimer emission as well as monomer emission. The emission characteristics of the dianthryldisilanes were compared with those of the corresponding anthrylpentamethyldisilanes (**1AS2Me**, **2AS2Me**, and **9AS2Me**). We also examined the time dependence of the fluorescence in view of the calculated potential energy surface of conformers in the ground state. The time constants correspond to the relaxation from the Franck–Condon structures those are most stable in the ground state to the relaxed excimer structures in the S_1 excited state.

1. Introduction

α,ω-Diaryl oligosilanes have attracted much attention because they have interesting photochemical characteristics compared to their carbon chain analogs [1–12]. 1,2-Di(9-anthryl)dimethylsilane is reported to produce unique [4+2] cycloadducts [3,4], which are very similar to the photochemical adducts produced from the 1,2-di(9-anthryl)ethylenes [13]. α,ω-Di(1-pyrenyl)oligosilanes were reported to show excimer emission by photoexcitation [6–8]. In that report, on the basis of the chemical shift of ^{1}H NMR spectra, two pyrenyl groups were proposed to interact even in the ground state, and a strong excimer emission was observed when the disilane unit acted as a linker. A charge transfer (CT) state of diaryloligosilanes formed in addition to the excimer formation in such cases [14–23].

Although the Si–Si bond is a single bond, it shows σ conjugation through σ orbital overlap. If a silane chain and two aromatic rings are connected, π orbitals of the aromatic rings can also conjugate with σ orbitals of the silane chain. In addition, the π orbitals of the two aromatic rings can spatially interact witheach other directly in the excited state, which is known as excimer. We have studied the photochemical properties of compounds composed of two aryl groups connected by a dimethylsilane chain – α,ω-di(1-naphthyl)oligosilanes, α,ω-di(9-anthryl)oligosilanes [2,9,11], and α-(9-anthryl)-ω-(1-naphthyl)oligosilanes [2,12]. Excimer emissions are observed for diaryloligosilanes, and CT emissions are observed in acetonitrile solutions of diaryloligosilanes that have longer silane linker units ($n > 4$).

A detailed experimental and theoretical investigation of the conformation of the intramolecular interactions of 1,2-diphenyltetramethyldisilane has been reported [24]. According to that study, intramolecular interactions in the HOMO originate between the phenyl π orbital and the disilane σ orbital (σ_{SiSi}–π_S) and those in the LUMO originate between the phenyl π* orbital and the disilane π* orbital (π^*_{SiSi}–$\pi_S{}^*$).

Intramolecular interaction between the anthryl group and the disilane unit essentially requires a perpendicular conformation between them because the overlap of the π orbital of the anthryl group and the σ orbital of the Si–Si chain is the origin of this interaction. We have investigated this phenomenon for **9A2S2**, in which the disilane unit is substituted at the 9 position of the anthryl group [9,11,12]. Therefore, steric hindrance between the hydrogen atoms at the 1 and 8 positions of the anthracene and disilane units was the external driving force behind this conformation, both in the ground state and the lowest excited singlet state.

* Corresponding author. Tel.: +81 43 290 3366.
E-mail address: karatsu@faculty.chiba-u.jp (T. Karatsu).

1010-6030/$ – see front matter © 2011 Elsevier B.V. All rights reserved.
doi:10.1016/j.jphotochem.2010.12.021

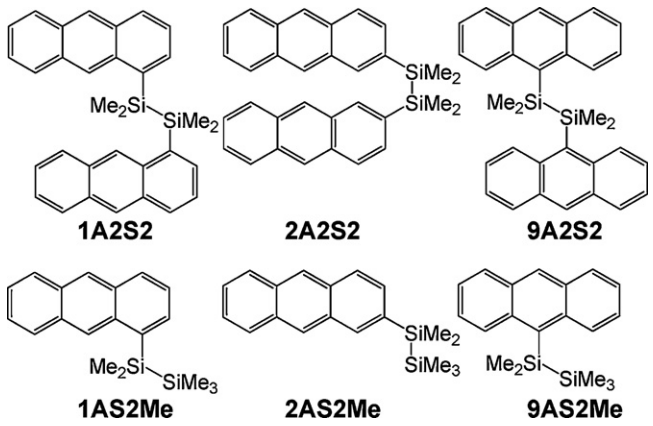

Fig. 1. Structures of anthryldisilanes examined.

In this study, we synthesized positionally isomeric 1,2-dianthryltetramethyldisilanes (**1A2S2** and **2A2S2**) and the corresponding anthrylpentamethyldisilanes (**1AS2Me**, **2AS2Me**, and **9AS2Me**), and investigated their photophysical properties by means of steady-state fluorescence spectroscopy and time-correlated single-photon counting methods (Fig. 1). **2A2S2** and, to a certain extent, **1A2S2** were free from their steric constraints and achieved increased conformational flexibility. We also attempted to understand the experimental observations by means of quantum chemical calculations.

2. Results and discussion

2.1. Calculated potential energy surfaces

The ground-state potential energy surfaces of the rotation around the dihedral angle C^{aryl}–Si–Si–C^{aryl} for **1A2S2**, **2A2S2**, and **9A2S2** were calculated by the B3LYP/6-31G* method, as shown in Fig. 2.

The disilane unit could assume a nearly perpendicular twisted conformation to the anthracene plane for **9A2S2** due to the steric hindrance between the silicon chain and the hydrogen atoms at the 1 and 8 positions of anthracene. The optimized structures for **9A2S2** were similar to the reported structure determined by X-ray single crystallography [25]. However, this conformation was caused by not only the steric effects but also the interaction between phenyl π orbital and disilane σ orbital (σ_{SiSi}–π_S). As shown in Fig. 3 and Table 1, the C^{aryl}–Si–Si bond angles in **1A2S2** and **2A2S2** had similar values to those in **9A2S2**. In addition, these values were almost independent of the dihedral angles. Rotation of the disilane unit around the C^{aryl}–Si bond had smaller amounts of steric hindrance in **1A2S2** and **2A2S2** than in **9A2S2**.

As mentioned above, the anthryl π orbital interacts with the disilane σ orbital (σ_{SiSi}–π_S). As shown in Fig. 3, there are isomers by the orientations of two anthryl groups in a molecule for **1A2S2** and **2A2S2**. In one isomer, the long axes of the two anthryl groups exhibit helical symmetry (Fig. 3a and d), and the other has non-helical symmetry (see Fig. 3b and c). The eclipsed conformer (a dihedral angle of 0°) of the former isomer has a structure such that the two anthryl groups could completely stack face to face, giving it mirror plane symmetry (C_s) between the Si–Si bonds. However, the eclipsed conformation of the latter isomer has a structure such that the two anthryl groups could stack on top of each other, and only one benzene ring in each anthryl group could stack face to face (C_2 symmetry). For simplicity, the former and latter series are expressed as anti and syn, respectively, in this paper. For syn-**1A2S2**, the energy minima are located at the ortho conformations (90° and −90°), and the maxima are located

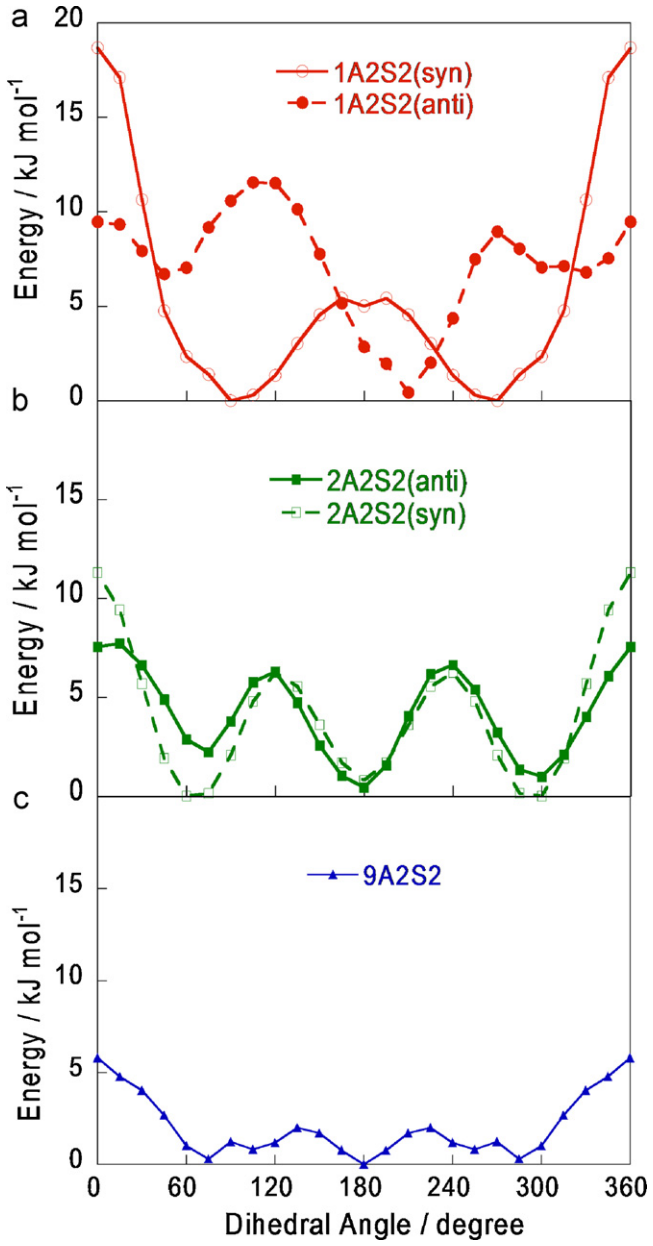

Fig. 2. Potential energy surfaces for the rotation of the dihedral angle of C^{Ant}–Si–Si–C^{Ant} of (a) **1A2S2**, (b) **2A2S2**, and (c) **9A2S2**, calculated with the DFT B3LYP/6-31G* method.

at the anti (5 kJ mol^{-1}) and the eclipsed (18 kJ mol^{-1}) conformations (Fig. 2a). This nomenclature of conformers was given in a previous report [26]. This shape of the potential energy surface is similar to that of **9A2S2**. On the other hand, the anti isomer has an energy minimum at the deviant (−150°) conformation. The energy maxima are located at the eclipsed and both ortho conformations (90° and 270°). In the potential energy surfaces of the conformations of **2A2S2**, there are almost no differences in energy between the anti (180°), gauche+ (60°), and gauche− (300°) conformers. The Si–C and Si–Si bonds are longer than a typical C–C bond, but the disilane unit has methyl groups as substituents. As a result, the activation energy for rotation around the Si–Si bond should be almost equivalent to the H_3C–CH_3 bond rotation energy.

We considered the structures of ground state stable conformers with the structures obtained by optimizations. The angles between the disilane unit and the anthracene plane are expressed

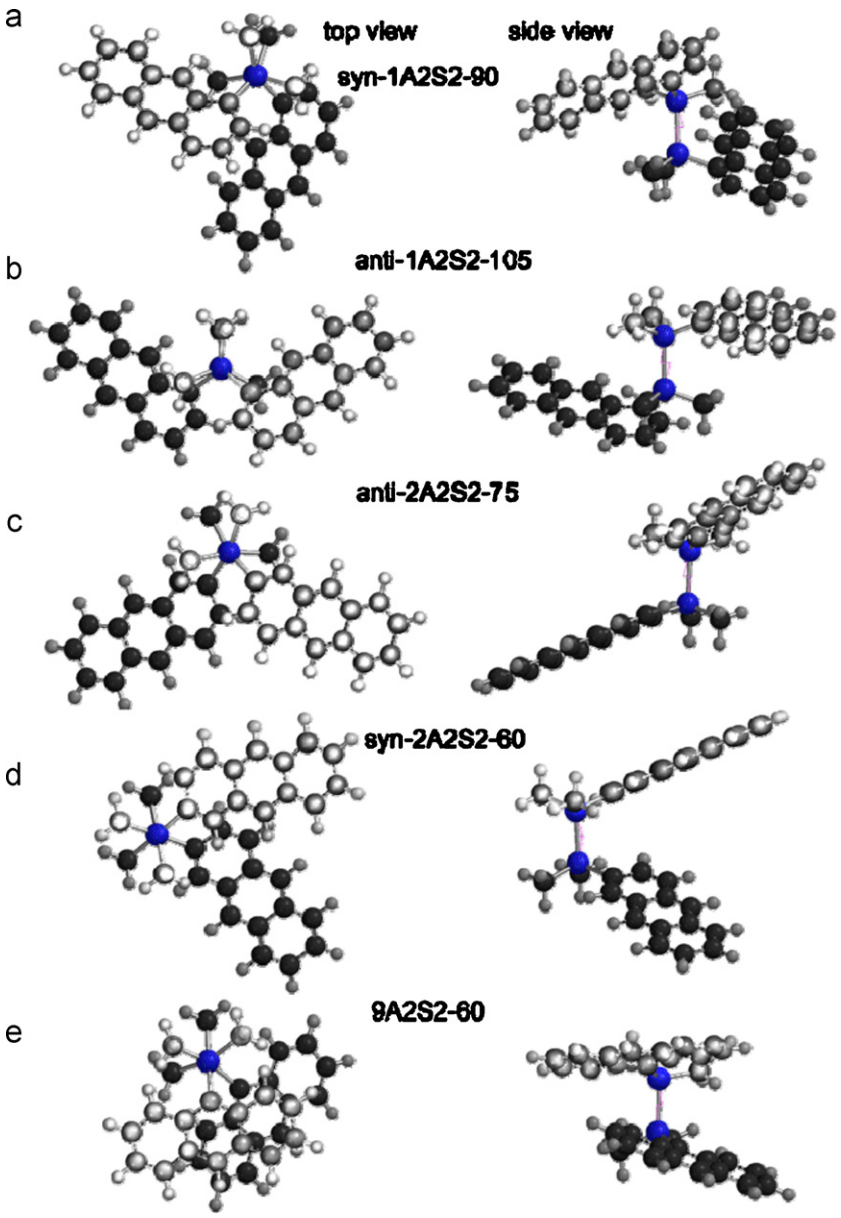

Fig. 3. Calculated structures of the most stable conformations of **1A2S2**, **2A2S2**, and **9A2S2** in their ground states (left side: top views, projection from the direction of the Si–Si bond; right side: side views). The digits after the compound abbreviations indicate the dihedral angles.

by the C^{Ant}–Si–Si bond angles and dihedral angles (C^{Ant}–C^{Ant}–Si–Si) of C^{9a}–C^{9}–Si–Si (**9A2S2**), C^{9a}–C^{1}–Si–Si (**1A2S2**), and C^{1}–C^{2}–Si–Si (**2A2S2**), as shown in Table 1. The C^{Ant}–Si–Si bond angles are about 110° and are almost independent of the conformations (see the third and fourth columns in Table 1). In addition to the C^{Ant}–Si–Si bond angles, the C^{Ant}–C^{Ant}–Si–Si dihedral angles are also tilted 15–25° from the perpendicular.

2.2. Conformations analyzed by chemical shifts of ^{1}H NMR spectra

Table 2 summarizes the chemical shifts of ^{1}H NMR spectra of the anthracene part of **1A2S2**, **2A2S2**, and **9A2S2** and **1AS2Me**, **2AS2Me**, and **9AS2Me**, along with that of normal anthracene as a reference. In general, most of the proton signals appear at the same chemical

Table 1
C^{Ant}–Si–Si bond angles and C^{Ant}–C^{Ant}–Si–Si dihedral angles for **9A2S2**, **1A2S2**, and **2A2S2**.

Compds.	Direction of two anthryl groups	C^{Ant}–Si–Si bond angle		C^{Ant}–C^{Ant}–Si–Si dihedral angles
		Most stable conformer (at dihedral angle of C^{Ant}–Si–Si–C^{Ant})	Conformer at dihedral angle C^{Ant}–Si–Si–C^{Ant} = 180°	
9A2S2	–	112.9 (60)	110.3	
1A2S2	Anti	110.1 (105)	107.3	70.4
	Syn	112.5 (90)	110.8	66.4
2A2S2	Anti	108.9 (60)	108.5	104.4
	Syn	110.3 (75)	108.9	104.4

Table 2
^{1}H NMR chemical shifts (δ: ppm) of anthracene, **1**, **2**, **9A2S2**, and **1**, **2**, **9AS2Me** in $CDCl_3$.

	H1	H2	H3	H4	H5	H6	H7	H8	H9	H10
Anthracene	7.98	7.44	7.44	7.98	7.98	7.44	7.44	7.98	8.40	8.40
1AS2Me	–	7.63	7.42	8.00	8.00	7.47	7.47	8.00	8.54	8.43
1A2S2	–	**7.33**	**7.33**	**7.56**	7.92	7.42	7.42	7.92	8.36	8.33
2AS2Me	8.10	–	7.49	7.98	7.98	7.45	7.45	7.98	8.41	8.39
2A2S2	**7.91**	–	7.44	**7.91**	8.00	7.44	7.44	8.00	8.38	**8.26**
9AS2Me	8.34	7.43	7.43	8.00	8.00	7.43	7.43	8.34	–	8.43
9A2S2	8.24	**7.13**	**7.35**	7.95	7.95	**7.35**	**7.13**	8.24	–	8.40

Bold and underlined numbers indicate shifts of signal toward a higher magnetic field than that of anthracene. Values of anthracene, **9AS2Me**, and **9A2S2** are taken from Refs. [18,6].

shift as that of anthracene. The substitution of a mono or a disilane unit moves chemical shifts of neighboring protons toward a lower magnetic field than that of anthracene (see the underlined numbers). In addition, three or four proton signals shift toward a higher magnetic field (see the bold and underlined numbers). These shifts were only observed for dianthryldisilanes, which have two anthryl units per molecule. Therefore, this shift is caused by the overlapping of two anthryl groups in the ground state. In addition, the effects of this shielding appear strongest in the 9 and 10 positions of anthracene because they have higher electron densities than the other carbon atoms. We determined the population of each conformer from the potential energy surface, and the ^{1}H NMR signals reflected the average population of the conformers at equilibrium.

Considering the overlapping of aromatic nuclei from the results of the magnetic shielding effects (H2 and H3 showed higher magnetic field shifts), one of the side benzene ring of two anthryl groups partially overlap each other in **9A2S2**. In addition, the chemical shifts of H6 and H7 are the same as those of H3 and H2, respectively. These similarities indicate that both of the side benzene rings of anthracene are under identical magnetic environment, and the conformer shown in Fig. 3e and its optical isomer are in rapid equilibrium along the potential energy surface of Fig. 2c. The H2, H3, and H4 protons of **1A2S2** appear at higher magnetic field than those of **1AS2Me** and anthracene. This fact better conforms to the syn conformer of Fig. 3a than the anti conformer of Fig. 3b. The anti conformer has a potential energy minimum at 210°, and the populations of the other conformers are limited (see the potential surface in Fig. 2a).

Similarly the H1, H4, and H10 protons of **2A2S2** appear at a higher magnetic field than those of **2AS2Me** and anthracene. These shifts correspond better to the overlap displayed by the syn conformer (Fig. 3d). The differences in the potential energy surfaces of the syn and anti conformers are small; however, the gauche conformers have slightly lower energies for the syn than for the anti conformer. Overall, potential energy surfaces calculated by the DFT method fit well with the results obtained by ^{1}H NMR.

2.3. Absorption spectra

Fig. 4 shows the absorption spectra of 1,2-dianthryltetramethyldisilanes and anthrylpentamethyldisilanes in cyclohexane. In Fig. 4a, we compared the absorption spectra of **2A2S2** and **2AS2Me** with those of 2-ethylanthracene (**2AC2H**) and anthracene. The absorption spectrum of **2AC2H** is very similar to that of anthracene, and the bathochromic shift is only a couple of nanometers. However, in the absorption spectra of **2A2S2** and **2AS2Me**, β-bands (^1B_b) around 360 nm are shifted about 10 nm to longer wavelengths compared to those of anthracene and 2-ethylanthracene [27,28]. We also observed these shifts for the p-bands (^1L_a) around 250 nm. Differences in the p-bands are much more apparent than those in the β-bands. The band shape is broadened for **2A2S2** and **2AS2Me**, and the longer absorption edge is extended to around 400 nm. This behavior is due to the interaction between the π orbital of the anthryl group and the π orbital of the disilane linker unit. This interaction must be affected by the substitution position. We compared the absorption spectra of the positionally isomeric anthryl disilanes for **1A2S2**, **1AS2Me**, **9A2S2**, **9AS2Me**, **2A2S2**, and **2AS2Me**. Fig. 4b shows the spectra of **1A2S2**, **9A2S2**, and **2A2S2**: the absorption spectra of **2A2S2** and **1A2S2** show a hypsochromic shift of about 15 nm compared with that of **9A2S2**. This is due partly to the interactions between the aromatic groups and the disilane unit and partly to the weak interaction between the two aromatic chromophores. In addition, the reviewer pointed out a possibility that the orientation of disilane unit along the transition moment of β-bands (short axis of anthracene) or p-bands (long axis of anthracene) affect on the position and ε of the absorption band. We determined these facts from the higher magnetic field shifts of the aromatic proton signals of the ^{1}H NMR, caused by a weak interaction between the two overlapping aromatic rings.

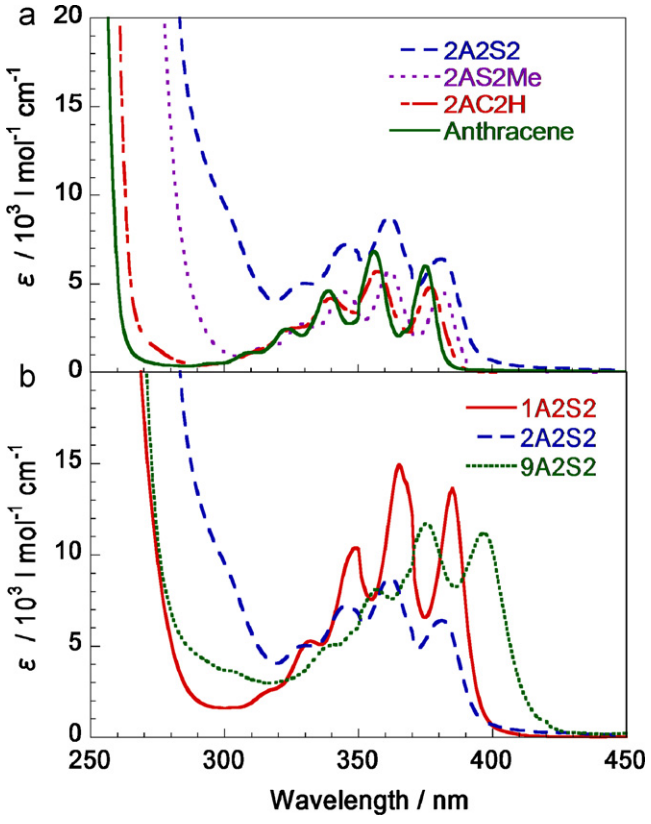

Fig. 4. UV–vis absorption spectra of (a) **2A2S2**, **2AS2Me**, **2AC2H**, and anthracene, and (b) **1A2S2**, **2A2S2**, and **9A2S2**, in c-hexane.

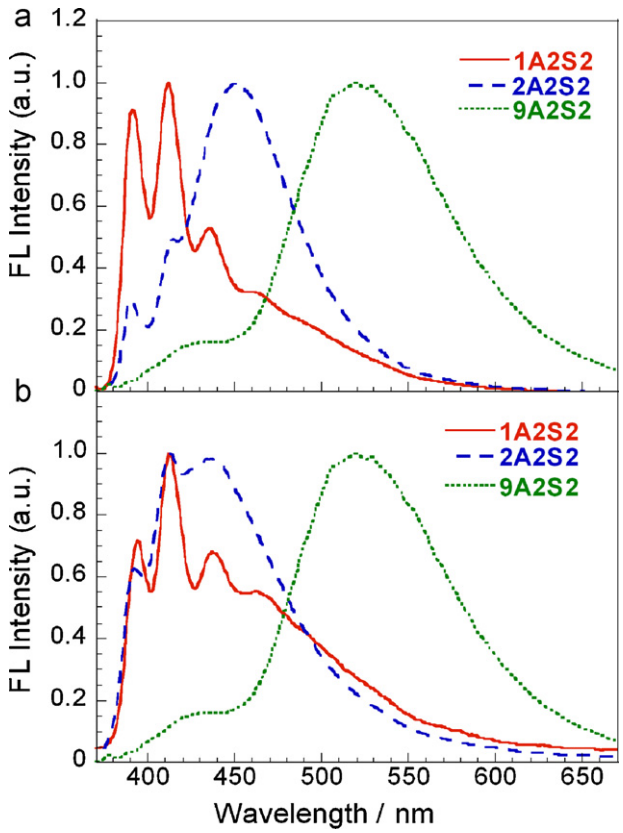

Fig. 5. Fluorescence spectra of dianthryltetramethyldisilanes (a) in c-hexane and (b) in acetonitrile purged by argon.

2.4. Fluorescence spectra and their quantum yields

Fig. 5a and b shows the fluorescence spectra of **1A2S2**, **2A2S2**, and **9A2S2** in cyclohexane and acetonitrile, respectively. Both short- and long-wavelength fluorescence were observed for disilanes having two anthryl groups (**1A2S2**, **2A2S2**, and **9A2S2**). The compounds **1AS2Me**, **2AS2Me**, and **9AS2Me**, in which each disilane has only one anthryl group, showed only monomer-like fluorescence (Fig. 6). **9AS2Me** has been reported to show broad structureless emission around 435 nm with lifetime τ = 12.8 ns [15]. This band shape is caused by a substitution of disilane unit along the transition moment of β-band. Therefore, these results suggest that the short- and long-wavelength fluorescence of **1A2S2**, **2A2S2**, and **9A2S2** are derived from monomer and excimer fluorescence, respectively, from the two anthryl rings. The solvents, such as cyclohexane (Fig. 5a) and acetonitrile (Fig. 5b), show only small effects on the spectral shape.

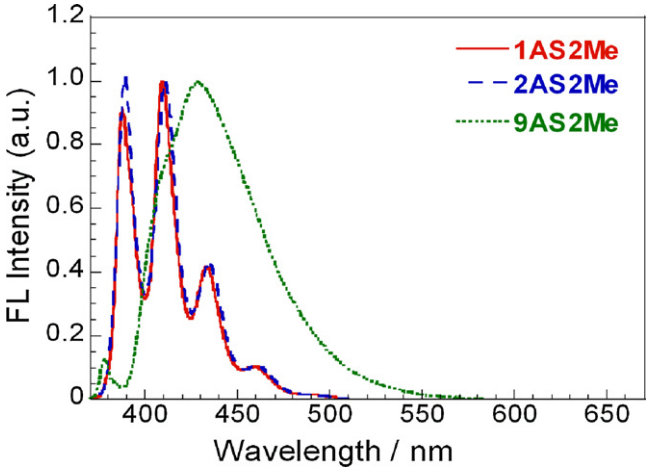

Fig. 6. Fluorescence spectra of anthrylpentamethyldisilanes in c-hexane purged by argon.

Excimers of 1,2-di(1-anthry)ethane (**1A2C2**) and 1,2-di(9-anthry)ethane (**9A2C2**) in which those two anthracene rings were connected by a carbon chain have been reported [29]. Excimer emissions were observed at 530 and 460 nm for **9A2C2** and **1A2C2**, respectively. In our case, the excimer formations of **9A2S2** and **1A2S2** appear at almost the same positions but with much stronger signals than those of the carbon chain analogs.

Compounds having a silicon chain length of more than 2 units (for the analogs of **9A2S2**) have been reported [11]; these compounds also show excimer emissions in cyclohexane. For n = 1–6, the fluorescence behavior was interesting. Excimer emission with a large Stokes shift was observed for **9A2S2** (n = 2, Fig. 5a). This shift (λ_{max} = 520 nm) is much larger than those observed for compounds with n = 3 and 4, indicating the closely stacked conformation of **9A2S2** in its excimer. Steric hindrance between the anthryl groups and the dimethylsilane chain unit may interrupt the conformation to produce the close stacking of the compounds with n = 3 and 4. In cyclohexane solutions, the **9A2S2** excimer emission was the most intense and the emission intensity decreased with increasing chain length.

The λ_{max} values of 620, 570, and 460 nm were reported for the excimer emission of anthracenophanes with 1, 2, and 3 phenyl rings, respectively, stacked face to face [30]. In addition, the Hirayama rule states that an excimer is most stable with a three-carbon chain unit. 1,3-Di(9-anthryl)propane undergoes efficient [4+4] cycloaddition, showing no excimer emission [31–33]. In our case, **9A2S2** has unique characteristics in which the Si–Si bond is longer than the C–C bond; the two anthracene rings stack like a sandwich with a large distance between the 9 and 9′ positions and a larger distance between the 10 and 10′ positions. The nearest distance between the 9 and 9′ positions is 3.55 Å according to the PM3 method; however, we recalculated the distances for the eclipsed conformation (0° dihedral angle) of the ground state as 3.99 Å (9–9′), 6.82 Å (10–10′), and 2.40 Å (Si–Si bond length) by the DFT method (B3LYP/6-31G*). Therefore, **9A2S2** has a strong excimer emission without undergoing efficient photocyclization. This may be attributed to two reasons: (1) a fairly long Si–Si bond length provides an appropriate distance between the two anthracene rings for excimer formation and (2) the conformation of the central Si–Si bond is restricted to gauche by the steric hindrance of the methyl substitutions on the Si atoms.

Positionally isomeric dianthryldisilanes studied in this work (**1A2S2** and **9A2S2**) have conformational isomers which have different intra-molecular orientations of two anthryl groups, and stacking area of two anthracene ring governs stability of intramolecular excimer, this area is expected to be in the order **9A2S2** > **1A2S2** > **2A2S2**. In addition, distance of two anthracene plane is also very important to consider stability of the excimer. For the eclipsed conformer of anti-**2A2S2**, distances between C2–C2′ and C4a–C4′a are 3.85 and 6.15 Å, respectively, with a 2.39 Å Si–Si bond length. These C2–C2′ and C4a–C4′ lengths are the distances between the ipso and para positions of the two silicon-substituted benzene rings, corresponding to the C9–C9′ and C10–C10′ distances, respectively, of **9A2S2**. Another syn eclipsed conformer has C2–C2′ and C4a–C4′a distances of 3.76 and 5.75 Å, respectively, with a 2.39 Å Si–Si bond length. Similarly for **1A2S2** (anti: C_s), C1–C1′ and C4–C4′ are 3.97 and 6.55 Å, respectively, with a 2.40 Å Si–Si bond length, and for **1A2S2** (syn: C_2), C1–C1′ and C4–C4′ are 3.90 and 6.16 Å, respectively, with a 2.39 Å Si–Si bond length. Mechanisms of the CT emission of aryl disilanes and oligosilanes in polar solvents

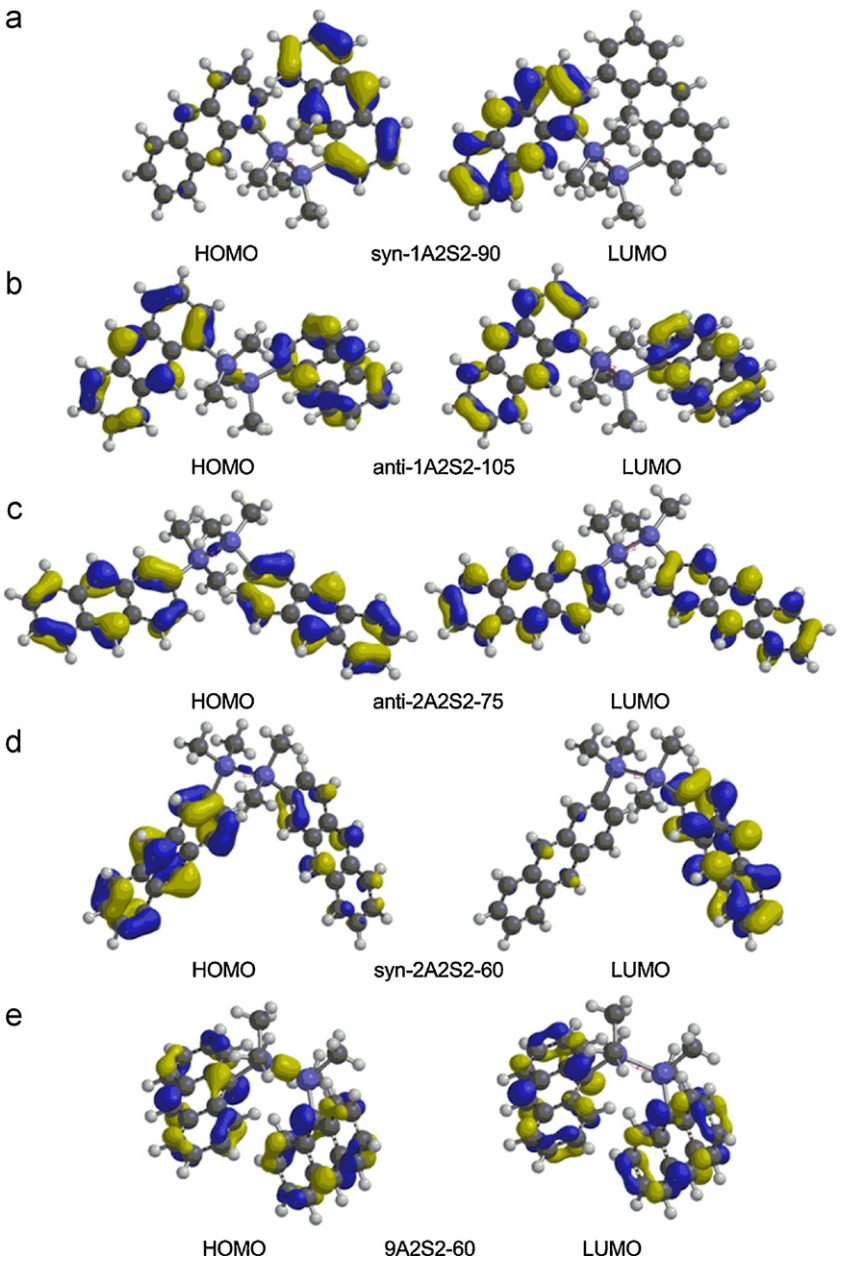

Fig. 7. HOMO and LUMO of **1A2S2** (a and b), **2A2S2** (c and d), and **9A2S2** (e) calculated for the structures presented in Fig. 3.

have been reported [11]. However, no anthryldisilanes examined in this study showed CT fluorescence.

Fig. 7 indicates HOMO–LUMO of conformers presented in Fig. 3. HOMO or LUMO delocalized on the two anthracene nuclei or localized on a one of the anthracene nucleus. In the latter case, MO having coefficient on another anthracene nucleus locates in energy nearly degenerated. The shape of HOMO and LUMO anthracene part is essentially same as those of HOMO and LUMO of anthracene itself. The coefficient of Si–Si linker part has higher in HOMO and almost negligible in LUMO. And sizes of these Si–Si MO are in the order of **9A2S2** > **1A2S2** > **2A2S2**, and this is same order as coefficient of ipso carbon atoms.

Table 3 lists the fluorescence quantum yields of 1,2-dianthryltetramethyldisilane and anthrylpentamethyldisilane in cyclohexane and acetonitrile. **1A2S2**, **2A2S2**, and **9A2S2** have lower fluorescence quantum yields (Φ_f) than the corresponding monoanthryldisilanes. (The dianthryldisilanes have 7.6%, 82%, and 10.5% of the Φ_f of the corresponding monoanthryldisilanes.) This trend

Table 3
Fluorescence properties of mono- and di-(1-, 2-, and 9-anthryl)disilanes.

	In c-hexane[a]			In acetonitrile[a]		
	λ_{max}^{LE} (nm)	λ_{max}^{EXM} (nm)	Φ_f	λ_{max}^{LE} (nm)	λ_{max}^{EXM} (nm)	Φ_f
Ant[b]	399	–	0.36		–	
1A2S2	412	470	0.04	412	471	0.005
1AS2Me	410	–	0.38	411	–	0.16
2A2S2	415	453	0.18	413	450	0.04
2AS2Me	411	–	0.22	412	–	0.08
9A2S2	425	520	0.07	425	524	0.07
9AS2Me	429	–	0.92	430	–	0.65

[a] Subscripts of LE and EXM indicate local and excimer fluorescence, respectively.
[b] Anthracene was used as a standard (Φ_f = 0.36; in cyclohexane).

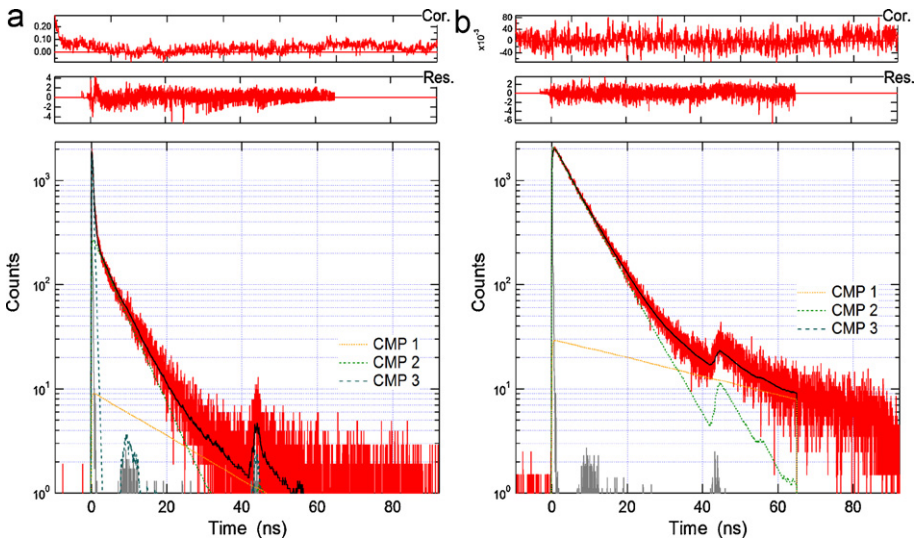

Fig. 8. Fluorescence time profile of **1A2S2** at (a) 440 and (b) 520 nm in c-hexane purged by argon.

might be caused by enhanced nonradiative deactivation through the excimer formation [34]. The energy difference between the excimer state and the ground state is smaller than that between the local excited singlet state and the ground state; therefore, vibrational coupling increases to promote nonradiative deactivation.

2.5. Time profiles of fluorescence

Figs. 8 and 9 show fluorescence time profiles of the dianthryldisilanes (**1A2S2** and **2A2S2**). As seen in the reported time profiles of **9A2S2**, the profiles show multiple-decay and rise plus multiple-decay time dependences at the local and the excimer fluorescence wavelength regions, respectively. For example, for **1A2S2**, triple decay profiles are composed of 0.354, 5.13, and 19.9 ns at 440 nm (Fig. 8a). On the other hand, we observed a rise component of 0.364 ns and double decay components of 6.28 and 47.2 ns at 520 nm (Fig. 8b). The fast decay observed at 440 nm and the rise component at 520 nm in a subpicosecond time scale are synchronized with each other (Table 4). This corresponds to the conversion from the local fluorescent conformer to the excimer.

The fastest components of **1A2S2** and **2A2S2** were compared with reported (in THF) and reexamined values (in cyclohexane) of **9A2S2**; the values were all in the subpicosecond region. The rate constants are in the order **9A2S2** > **1A2S2** > **2A2S2**. This is explained by the difference of the local fluorescent structure of the stable conformer, which might assume a similar conformation to that of the ground state, and structures of the excimer, the $\pi-\pi$ stacking conformation, in the positionally isomeric dianthryldisilanes. The ground state molecules are in equilibrium in the ground state potential energy surface and distributed according to the Boltzmann distribution law. According to the Franck–Condon principle, molecules excite to the singlet excited state retaining their structures. Then, the molecules relax to the stabilized structure of the excited state, i.e., an excimer. The time-dependent fluorescence spectra essentially reflect these changes in the conformation. In the case of **9A2S2**, the 82.1 ps decay at 420 nm and the 74.4 ps rise at 520 nm reflect small or quick structural changes of the ground state to the excited state structures. It is not always true that large Stork's shift reflects large conformational change. A large Stork's shift may bring by a strong interaction between the chromophores even this process is caused by a small conformational change. In the case of **1A2S2**, time constants of the decay and rise are 354 and 364 ps, respectively, and these times are much larger than those of **9A2S2**. In the case of **2A2S2**, time constants of the decay and rise are 654 and 461 ps, respectively (Fig. 9a and b). The second and third components may reflect the decays of the local and excimer fluo-

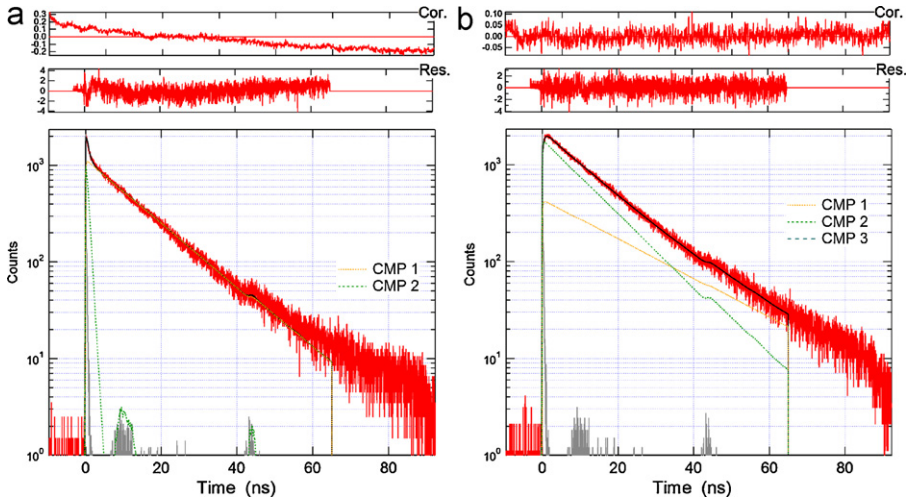

Fig. 9. Fluorescence time profile of **2A2S2** at (a) 440 and (b) 520 nm in c-hexane purged by argon.

Table 4
Time constants of decay and rise components (expressed as nano-second) of the fluorescence of 1,2-(1,1′-, 2,2′-, or 9,9′-dianthryl)-tetramethyldisilanes in c-hexane purged by argon.

	τ (λ_{obs} (nm))	τ (λ_{obs} (nm))
1A2S2	0.354 + 5.13 + 19.9 (440)	−0.364 + 6.28 + 47.2 (520)
2A2S2	0.654 + 12.7 (440)	−0.461 + 11.0 + 20.8 (520)
9A2S2[a]	0.0821 + 0.248 + 7.76 (420)	−0.0744 + 0.260 + 7.30 (520)

[a] 0.0998 + 5.07 + 20.6 (420 nm) and −0.0850 + 5.32 + 19.1 (520 nm) in THF in Ref. [11].

rescence, respectively. The large intensity of the fast component of **1A2S2** at 440 nm is due to the small contribution of the excimer fluorescence at this wavelength.

The weak excimer fluorescence of **1A2S2** is explained by the small population of the conformers of the excimer in equilibrium with the ground state. The syn-**1A2S2** isomer has energy minima in its ortho conformations (90° and 270°), and anti-**1A2S2** has an energy minimum at 210°. The gauche+ and gauche− conformations have very high energies. Also, the eclipsed conformation of syn-**1A2S2** has a very high potential energy (18 kJ mol^{-1}). In addition, the wavelength of the excimer fluorescence maximum reflects the strong intramolecular interactions within the excimer. We understand these energies are dependent on two factors: the first is the overlapping area in the stacking of the two anthracene rings, and the second is the angle of Si–Si–C (ipso carbon of anthracene rings). The tilting angle between two anthracene planes in the excimer is also very important. These two factors are dependent on the substitution position of anthracene.

3. Conclusions

We calculated the ground state potential energy surfaces for the rotamers of positionally isomeric dianthrylteteramethyldisilanes with the DFT method and measured the stationary states and time-resolved fluorescence spectra. Their photophysical properties were explained by the excitations of the stable conformers in the ground state and the formations of excimers in the singlet excited state. Rate constants of the formation of the excimers from the Franck–Condon state, which reflect the population of conformers in the ground state equilibrium, are in the order **9A2S2** > **1A2S2** > **2A2S2**, and the maximum wavelengths of excimer fluorescence are also in the same order, corresponding to the better stacking of the two anthryl moieties in a molecule.

4. Experimental

4.1. Spectroscopic apparatus

We prepared sample solutions in cyclohexane, THF, and acetonitrile (Kanto Chemical), and deoxygenated them by bubbling highly purified argon (>99.999%) through a needle. Absorption spectra were recorded with a JASCO V-570 spectrophotometer. Steady-state fluorescence spectra were measured with a JASCO FP-6600 fluorimeter using a 1 cm × 1 cm quartz cuvette. We performed time-dependent fluorescence measurements by the time-correlated single-photon counting method. The apparatus was assembled based on our previous paper [35,36]. Excitation at 410 nm was achieved using a diode laser (PicoQuant, LDH-P-C-405) with a power control unit (PicoQuant, PDL 800-B) having a repetition rate of 2.5 MHz. Temporal profiles of the fluorescence decay were recorded using a microchannel plate photomultiplier (Hamamatsu, R3809U) equipped with a Time correlated single photon counting (TCSPC) computer board module (Becker and Hickl, SPC630). The instrument response function had a full width at half maximum of 51 ps. The values of χ^2 and the Durbin–Watson parameters, obtained by nonlinear regression, were used as criteria for the best fit [37].

4.2. Synthesis

Synthetic methods for **9A2S2** and **9AS2Me** were reported previously [11,38,39]. We prepared **1A2S2** and **2A2S2** from 1- and 2-anthryllithium (obtained from aryl bromide and 1.6 M *n*-butyllithium in hexane), respectively, and 1,2-dichlorotetramethyloligosilane purchased from Tokyo Kasei. Chloropentamethyldisilane was purchased from Aldrich. **1AS2Me** and **2AS2Me** were prepared from 1- and 2-anthryllithium (obtained from aryl bromide and 1.6 M *n*-butyllithium in hexane), respectively, and chloropentamethyldisilane. 1- and 2-Bromoanthracene were prepared using 1- and 2-aminoanthraquinone, respectively, by the method reported [40–42]. All of the compounds were characterized using a JEOL SX-400 ^{1}H NMR spectrometer.

1A2S2 ^{1}H NMR (400 MHz, $CDCl_3$) δ = 8.36 (s, 2H, Ar–H), 8.33 (s, 2H, Ar–H), 7.94–7.90 (m, 4H, Ar–H), 7.56 (dd, J = 6.6 Hz, 1.2 Hz, 2H, Ar–H), 7.44–7.40 (m, 4H, Ar–H), 7.36–7.31 (m, 4H, Ar–H), 0.58 (s, 12H, $-CH_3$).

FAB-MS: m/z = 470 (M^+)

1AS2Me ^{1}H NMR (400 MHz, $CDCl_3$) δ = 8.54 (s, 1H, Ar–H), 8.43 (s, 1H, Ar–H), 8.02–7.98 (m, 3H, Ar–H), 7.63 (dd, J = 6.6 Hz, 1.2 Hz, 1H, Ar–H), 7.49–7.45 (m, 4H, Ar–H), 7.42 (dd, J = 6.6 Hz, 8.6 Hz, 1H, Ar–H), 0.57 (s, 6H, $SiMe_2$), 0.12 (s, 9H, $SiMe_3$).

GC–MS m/z = 308 (M^+)

2A2S2 ^{1}H NMR (400 MHz, $CDCl_3$) δ = 8.38 (s, 2H, Ar–H), 8.26 (s, 2H, Ar–H), 8.01–7.99 (m, 4H, Ar–H), 7.93–7.89 (m, 4H, Ar–H), 7.48–7.41 (m, 6H, Ar–H), 0.48 (s, 12H, $-CH_3$).

FAB-MS: m/z = 470 (M^+)

2AS2Me ^{1}H NMR (400 MHz, $CDCl_3$) δ = 8.41 (s, 1H, Ar–H), 8.39 (s, 1H, Ar–H), 8.10 (s, 1H, Ar–H), 8.02–7.94 (m, 3H, Ar–H), 7.49 (dd, J = 8.6 Hz, 1.0 Hz, 1H, Ar–H), 7.47–7.43 (m, 2H, Ar–H), 0.45 (s, 6H, $SiMe_2$), 0.10 (s, 9H, $SiMe_3$).

GC–MS m/z = 308 (M^+)

4.3. Calculation

Calculations using DFT method B3LYP/6-31G* level were performed by a Spartan'06 and *Gaussian* 03 [43].

Acknowledgments

Authors thank Analytical Center of Chiba University for her help of chemical analyses of the compounds. This work was supported by Grants-in-Aids for Scientific Research (No. 20550056) and G-COE program from the Ministry of Education, Culture, Sports, Science and Technology (MEXT), and G-COE kick-off program from Chiba University.

References

[1] R.D. Miller, J. Michl, Polysilane high polymers, Chem. Rev. 89 (1989) 1359–1410.
[2] T. Karatsu, Photochemistry and photophysics of organomonosilane and oligosilanes: updating their studies on conformation and intramolecular interactions, J. Photochem. Photobiol. C: Photochem. Rev. 9 (2008) 111–137.
[3] H. Sakurai, K. Sakamoto, A. Nakadaira, M. Kira, Photochemistry of di(9-anthryl)dimethyl-silane and -germane, Chem. Lett. 14 (1985) 497–498.
[4] M. Daney, C. Vanucci, J.-P. Desvergne, A. Castellan, H. Bouas-Laurent, Photochemistry of bichromophoric systems. Silicon guided intramolecular 9,10,1′,2′ anthracene photodimerization in bis(9-anthryl) dimethylsilane, Tetrahedron Lett. 26 (1985) 1505–1508.
[5] C.G. Pitt, R.N. Carey, E.C. Toren Jr., Nature of the electronic interactions in aryl-substituted polysilanes, J. Am. Chem. Soc. 94 (1972) 3806–3811.
[6] D. Declercq, P. Delbeke, F.C. de Schryver, L.V. Meervelt, R.D. Miller, Ground- and excited-state interaction in di-1-pyrenyl-substituted oligosilanes, J. Am. Chem. Soc. 115 (1993) 5702–5708.

[7] D. Declercq, F.C. de Schryver, R.D. Miller, Fluorescence behaviour of pyrene substituted tri- and hexa-silanes, Chem. Phys. Lett. 186 (1991) 467–473.
[8] D. Declercq, E. Hermans, F.C. de Schryver, R.D. Miller, Photophysics of pyrene substituted oligosilanes, Proc. Indian Acad. Sci., Chem. Sci. 105 (1993) 451–461.
[9] T. Karatsu, T. Shibata, A. Nishigaki, K. Fukui, A. Kitamura, π–π and σ–π Interactions in α,ω-dinaphthyl and -dianthryl oligosilanes in solution, Chem. Lett. (2001) 994–995.
[10] M.-C. Fang, A. Watanabe, M. Matsuda, Emission spectra of σ–π-conjugated organosilicon copolymers consisting of alternating dimethylsilylene and aromatic units, Macromolecules 29 (1996) 6807–6813.
[11] T. Karatsu, T. Shibata, A. Nishigaki, A. Kitamura, Y. Hatanaka, Y. Nishimura, S. Sato, I. Yamazaki, π–π and σ–π Interactions in α,ω-di-(9-anthryl) and di-(1-naphthyl) oligosilanes studied by time-resolved fluorescence in solution, J. Phys. Chem. B 107 (2003) 12184–12191.
[12] T. Karatsu, M. Terasawa, S. Yagai, A. Kitamura, T. Nakamura, Y. Nishimura, I. Yamazaki, Time-resolved fluorescence of α-(9-anthryl)-ω-(1-naphthyl)-oligosilanes: intramolecular electronic energy and charge transfer through π–π and σ–π interactions, J. Organomet. Chem. 689 (2004) 1029–1035.
[13] H.-D. Becker, Excited state reactivity and molecular topology relationships in chromophorically substituted anthracenes, in: D.H. Volman, G.S. Hammond, K. Gollnick (Eds.), Advances in Photochemistry, 15, Wiley & Sons, New York, 1990, pp. 139–227.
[14] C.G. Pitt, R.N. Carey, E.C. Toren Jr., J. Am. Chem. Soc. 94 (1972) 3806.
[15] H. Shizuka, Y. Sato, Y. Ueki, M. Ishikawa, M. Kumada, The $2p\pi^* \rightarrow 3d\pi$ interaction in aromatic silanes, J. Chem. Soc., Faraday Trans. 1 (80) (1984) 341–357.
[16] H. Shizuka, K. Okazaki, M. Tanaka, M. Ishikawa, M. Sumitani, K. Yoshihara, Intramolecular $2p\pi^* \rightarrow 3d\pi$ charge transfer in the excited state of phenyldisilane studied by picosecond and nanosecond laser spectroscopy, Chem. Phys. Lett. 113 (1985) 89–92.
[17] M. Yamamoto, T. Kudo, M. Ishikawa, S. Tobita, H. Shizuka, Experimental and theoretical studies on the intramolecular charge-transfer emission of phenyldisilanes, J. Phys. Chem. A 103 (1999) 3144–3154.
[18] K.A. Horn, R.B. Grossman, J.R.G. Throne, A.A. Whitenack, σ,π* Charge-transfer excited states of substituted (phenylethyny1)pentamethyldisilanes, J. Am. Chem. Soc. 111 (1989) 4809–4821.
[19] M. Kira, T. Miyazawa, H. Sugiyama, M. Yamaguchi, H. Sakurai, σ,π* Orthogonal intramolecular charge-transfer (OICT) excited states and photoreaction mechanism of trifluoromethyl-substituted phenyldisilanes, J. Am. Chem. Soc. 115 (1993) 3116–3124.
[20] H. Sakurai, H. Sugiyama, M. Kira, Dual fluorescence of aryldisilanes and related compounds. Evidence for the formation of $^1(\sigma\pi^*)$ orthogonal intramolecular charge-transfer states, J. Phys. Chem. 94 (1990) 1837–1843.
[21] Y. Tajima, H. Ishikawa, T. Miyazawa, M. Kira, N. Mikami, First observation of intramolecular charge-transfer emission from jet-cooled (p-cyanophenyl)pentamethyldisilane in an isolated molecular condition, J. Am. Chem. Soc. 119 (1997) 7400–7401.
[22] H. Sakurai, M. Kira, Charge-transfer spectra of some phenyl and naphthyl derivatives. Relative importance of σ–π and n–π conjugation involving the π Si–Si system, J. Am. Chem. Soc. 96 (1974) 791–794.
[23] H. Sakurai, M. Kira, Charge-transfer spectra of some para-substituted phenylpentamethyldisilanes. Substituent effects on the relative intensities of two charge-transfer bands, J. Am. Chem. Soc. 97 (1975) 4879–4883.
[24] H. Tsuji, Y. Shibano, T. Takahashi, M. Kumada, K. Tamao, Conformation dependence of photophysical properties of σ–π conjugation as demonstrated by cis- and trans-1,2-diaryl-1,2-disilacyclohexane cyclic systems, Bull. Chem. Soc. Jpn. 78 (2005) 1334–1344.
[25] D.-D.H. Yang, N.C. Yang, I.M. Steele, H. Li, Y.-Z. Ma, G.R. Fleming, Photochemistry of dianthrylsilanes: a study of σ,π*-interaction, J. Am. Chem. Soc. 125 (2003) 5107–5110.
[26] J. Michl, R. West, Conformations of linear chains. Systematics and suggestions for nomenclature, Acc. Chem. Res. 33 (2000) 821–823.
[27] J.B. Birks, Photophysics of Aromatic Molecules, Wiley Interscience, London, 1970.
[28] M. Montalti, A. Credi, L. Prodi, M.T. Gandolfi, Handbook of Photochemistry, CRC Press, Boca Raton, FL, USA, 2006.
[29] H. Bouras-Laurent, J.-P. Desvergne, in: H. Photochromism, H. Dürr, Bouras-Laurent (Eds.), Cycloaddition reactions involving 4n electrons: (4+4) cycloaddition reactions between unsaturated conjugated systems, Elsevier, Amsterdam, 1990, pp. 561–630 (Chapter 14, and references therein).
[30] T. Hayashi, N. Mataga, Y. Sakata, S. Misumi, M. Morita, J. Tanaka, Excimer fluorescence and photodimerization of anthracenophanes and 1,2-dianthrylethanes, J. Am. Chem. Soc. 98 (1976) 5910–5913.
[31] F. Hirayama, Intramolecular excimer formation I. Dipheyl and triphenyl alkanes, J. Chem. Phys. 42 (1965) 3163–3171.
[32] H. Bouas-Laurent, A. Castellan, J.-P. Desvergne, From anthracene photodimerization to jaw photochromic materials and photocrowns, Pure Appl. Chem. 52 (1980) 2633–2648.
[33] W.R. Bergmark, G. Jones II., Th.E. Reinhardt, A.M. Halpern, Photoisomerization of bis(9-anthry1)methane and other linked anthracenes. The role of excimers and biradicals in photodimerization, J. Am. Chem. Soc. 100 (1978) 6665–6673.
[34] J.L. Charlton, R. Dabestani, J. Saltiel, Role of triplet–triplet annihilation in anthracene dimerization, J. Am. Chem. Soc. 105 (1983) 3473–3476.
[35] I. Yamazaki, N. Tamai, H. Kume, H. Tsuchiya, K. Oba, Microchannel-plate photomultiplier applicability to the time-correlated photon-counting method, Rev. Sci. Instrum. 56 (1985) 1187–1194.
[36] Y. Nishimura, M. Kamada, M. Ikegami, R. Nagahata, T. Arai, The relaxation dynamics of the excited state of stilbene dendrimers substituted with phenylacetylene groups, J. Photochem. Photobiol. A: Chem. 178 (2006) 150–155.
[37] N. Boens, N. Tamai, I. Yamazaki, T. Yamazaki, Picosecond single photon timing measurements with a proximity type microchannel plate photomultiplier and global analysis with reference convolution, Photochem. Photobiol. 52 (1990) 911–917.
[38] H. Gilman, S. Inoue, The preparation of some α,ω-dichloro permethylated polysilanes, J. Org. Chem. 29 (1964) 3418–3419.
[39] M. Kumada, M. Yamaguchi, Y. Yamamoto, J. Nakajima, K. Shiina, Synthesis of some methyldisilanes containing functional groups, J. Org. Chem. 21 (1956) 1264–1268.
[40] R.S. Coleman, M.A. Mortensen, Stereocontrolled synthesis of anthracene β-C-ribosides: fluorescent probes for photophysical studies of DNA, Tetrahedron Lett. 44 (2003) 1215–1219.
[41] M.P. Doyle, B. Siegfried, J.F. Dellaria, Alkyl nitrite-metal halide deamination reactions. 2. Substitutive deamination of arylamines by alkyl nitrites and copper(II) halides. A direct and remarkably efficient conversion of arylamines to aryl halides, J. Org. Chem. 42 (1977) 2426–2431.
[42] T.R. Criswell, B.H. Klanderman, Studies related to the conversion of 9,10-anthraquinones to anthracenes, J. Org. Chem. 39 (1974) 770–774.
[43] M.J. Frisch, G.W. Trucks, H.B. Schlegel, G.E. Scuseria, M.A. Robb, J.R. Cheeseman, J.A. Montgomery Jr., T. Vreven, K.N. Kudin, J.C. Burant, J.M. Millam, S.S. Iyengar, J. Tomasi, V. Barone, B. Mennucci, M. Cossi, G. Scalmani, N. Rega, G.A. Petersson, H. Nakatsuji, M. Hada, M. Ehara, K. Toyota, R. Fukuda, J. Hasegawa, M. Ishida, T. Nakajima, Y. Honda, O. Kitao, H. Nakai, M. Klene, X. Li, J.E. Knox, H.P. Hratchian, J.B. Cross, C. Adamo, J. Jaramillo, R. Gomperts, R.E. Stratmann, O. Yazyev, A.J. Austin, R. Cammi, C. Pomelli, J.W. Ochterski, P.Y. Ayala, K. Morokuma, G.A. Voth, P. Salvador, J.J. Dannenberg, V.G. Zakrzewski, S. Dapprich, A.D. Daniels, M.C. Strain, O. Farkas, D.K. Malick, A.D. Rabuck, K. Raghavachari, J.B. Foresman, J.V. Ortiz, Q. Cui, A.G. Baboul, S. Clifford, J. Cioslowski, B.B. Stefanov, G. Liu, A. Liashenko, P. Piskorz, I. Komaromi, R.L. Martin, D.J. Fox, T. Keith, M.A. Al-Laham, C.Y. Peng, A. Nanayakkara, M. Challacombe, P.M.W. Gill, B. Johnson, W. Chen, M.W. Wong, C. Gonzalez, J.A. Pople, Gaussian 03, Revision B. 03, Gaussian, Inc., Pittsburgh, PA, 2003.